

PITCH-ANGLE SCATTERING OF ENERGETIC PARTICLES IN THE CURRENT SHEET OF THE MAGNETOSPHERIC TAIL AND STATIONARY DISTRIBUTION FUNCTIONS

N. A. TSYGANENKO

Institute of Physics, Leningrad State University, Leningrad 198904, U.S.S.R.

(Received 13 August 1981)

Abstract—An investigation of pitch-angle scattering of energetic particles in magnetic field configurations with a current sheet similar to that observed in the geomagnetotail has been performed. The magnetic field model is specified by two parameters which are the current sheet thickness in units of particle gyroradius and the angle between the magnetic field lines and the sheet plane. Computations of a considerable number of trajectories (about 20,000 for each model case) has provided the possibility of obtaining the matrix of pitch-angle scattering and the corresponding kernel function of the integral equation for the stationary particle distribution function. Solution of this equation shows that isotropic distributions are formed only in the case of a sufficiently thick current sheet. Particle scattering in a thin field reversal region leads to the formation of an anisotropic stationary distribution. The results can be used for interpretation of the data on the spatial distribution of energetic particle fluxes in the near part of the magnetospheric tail and in the vicinity of the outer boundary of the radiation belt.

1. INTRODUCTION

The question of the validity of the adiabatic approximation for studies of particle motion in the nightside magnetosphere has at least two aspects. The first is related to a problem of the plasma sheet formation and balance of magnetic and mechanical stresses in the magnetotail, since the details of particle motion near the current sheet determine the velocity distribution function and, hence, a degree of plasma pressure anisotropy and its spatial gradients (Tsyganenko, 1975, 1981; Shabansky, 1971). The second aspect concerns the possibility of using the measurements of energetic particle fluxes as a diagnostic tool for studies on the general configuration of the geomagnetic field and details of its structure. A typical example of such an approach is the work by West *et al.* (1978), which shows the possibility of constructing an "instantaneous" magnetic field model for the near tail region, based on data on the angular distribution of energetic electron fluxes. In this paper an assumption has been introduced, that a non-adiabatic motion of particles in the plasma sheet should cause a strong pitch-angle scattering and, as a result, a rapid relaxation of the angular distribution to isotropy. The last conclusion, however is not evident *a priori*, because the scattering may be different for particles with different initial pitch angles and, hence, the stationary distribution function in the magnetotail field line

tubes can be anisotropic in the general case. The aim of the present paper is to clarify this question. Using results of numerical trajectory computations, the efficiency of particle scattering is investigated for different model parameters and the stationary distribution functions are then calculated.

2. SCATTERING MATRIX AND ITS RELATION TO STATIONARY PITCH-ANGLE DISTRIBUTION FUNCTION

Consider a stationary beam of particles with different pitch angles, incident upon the magnetic field reversal region, say, from below, as it is shown in Fig. 1. After having done a complicated motion near the reversal region, a certain portion of the beam particles will be eventually ejected away from the opposite side of the sheet, and the rest of the particles will be reflected back. In both cases the initial pitch angle of each particle, θ_i , will be changed to its final value, θ_f , which depends on θ_i , as well as on initial gyration phase, φ_i , specified at the point of trajectory intersection with a certain reference plane orthogonal to the magnetic field line (see Fig. 1).

It is more convenient to deal with quantities $\mu_i = \sin^2 \theta_i$ and $\mu_f = \sin^2 \theta_f$, rather than with pitch angles. Let us define a function $S(\mu_f, \mu_i)$ representing a density of scattered particles distribution in the quantity μ_f for different initial values of μ_i , assuming the initial distribution in φ_i

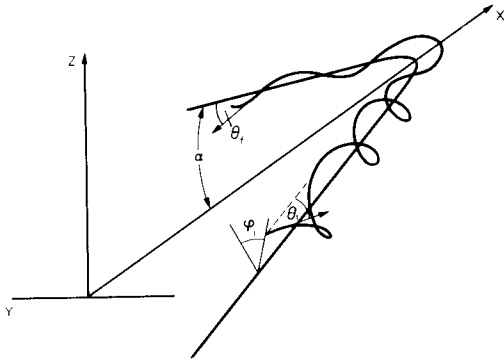


FIG. 1. A SKETCH OF THE SCATTERING PARTICLE TRAJECTORY (THE FORMULATION OF THE PROBLEM).

to be uniform. The last assumption enables us to represent the particle distribution by means of function $f(\theta)$ containing only the pitch-angle dependence. The flux of incident particles having pitch angles inside the interval $(\theta_i, \theta_i + d\theta_i)$ is

$$2\pi v_i f(\theta_i) \sin \theta_i d\theta_i = 2\pi v f(\theta_i) \cos \theta_i \sin \theta_i d\theta_i \\ = \pi v f(\theta_i) d\mu_i$$

and the flux of scattered particles in the outgoing beam inside the interval $(\mu_f, \mu_f + d\mu_f)$ is

$$dF = \pi v d\mu_f \int_0^1 S(\mu_f, \mu_i) f(\theta_i) d\mu_i \quad (1)$$

We neglect electric fields and, hence, the particle velocity v is assumed to remain constant during the scattering act.

As has been noted above, the incident beam is divided into penetrating and reflected beams. However, in case of symmetrical magnetic field and plasma configuration it is natural to assume that there exist two identical beams which impinge the reversal region from both sides and also produce a pair of identical reflected beams. Therefore, it is convenient to assume that all particles from the incident beam (hereafter—the beam 1) penetrate into the upper half-space and form the scattered beam 2. We shall assume also, that the magnetic field outside the reversal region does not differ considerably from being uniform, so that particles move here adiabatically and their mirror points are located far enough from the scattering zone. If we neglect the precipitation of particles in the ionospheric loss cone, then the beam 3, which returns back to the reversal from mirror points,

should have the same pitch-angle distribution as that in the beam 2. The phase grouping of particles, which is possible in the beam 2 (near the exit from the reversal region), must be absent in the beam 3 because of a phase mixing on the long way to mirror points and back to the sheet. On the other hand, the steady state and symmetry of the whole system requires that the beam 3 to be identical to initial beam 1. Therefore, equating the corresponding differential fluxes, we obtain on taking account of (1) and the definition of $S(\mu_f, \mu_i)$:

$$f(\theta_f) = \int_0^1 S(\mu_f, \mu_i) f(\theta_i) d\mu_i \quad (2)$$

The stationary distribution function $f(\theta)$ can be thus found as a solution of the integral equation (2). The kernel function $S(\mu_f, \mu_i)$ can be obtained from computations of a large number of particle trajectories with values of μ_i distributed in small intervals $(\mu_i, \mu_i + \Delta\mu)$ and with uniform distribution in phase φ_i . Scattering matrix elements $S_{ki} \equiv S(\mu_f^k, \mu_i^i)$ are then defined as relative filling densities of intervals $(\mu_f^k, \mu_f^k + \Delta\mu)$ in the scattered beam.

3. MAGNETIC FIELD MODEL

The following model magnetic field distribution was adopted for our numerical analysis

$$B_x(z) = \begin{cases} (B_{x0}/d^2)z(2d - |z|) & |z| \leq d \\ B_{x0} \text{sign}(z) & |z| \geq d \end{cases} \quad (3) \\ B_z = \text{const.}$$

The B_x -component is an odd continuous function of z having also a continuous derivative. Outside the field reversal region ($|z| > d$) the magnetic field is uniform. The simplicity of model formulas (3) permits rapid computation of a considerable number of trajectories. This is an important feature, bearing in mind that our aim is to calculate the scattering matrix elements with a sufficient accuracy.

The equations of the particle motion, like in the paper of Wagner *et al.* (1979), were transformed to dimensionless form by introducing Larmor units of length $r_L = mvc/eB_0$ and time $t_L = \omega_L^{-1} = r_L/v$; quantity B_0 refers to the region outside the reversal and serves as the unit of the magnetic field. In such a formulation on the problem has only two independent parameters which specify completely a model version: (i) the angle between the magnetic field lines outside the reversal region and the current sheet plane $\alpha = \sin^{-1}(B_z/B_0)$, and (ii) the dimensionless current sheet thickness

$$\beta = d/r_{Lz} = (d/r_L) \sin \alpha.$$

Owing to the absence of x - and y -dependence in the magnetic field model, two additional integrals of motion can be applied which enables the number of differential equations to be reduced. After having introduced the dimensionless variables, we arrive finally at the following set of equations

$$\begin{aligned}\dot{x} &= yB_z + C_1 \\ \dot{y} &= A(x,z) + C_2 \\ \dot{z} &= v_z \\ \dot{v}_z &= -[A(x,z) + C_2]B_x(z),\end{aligned}$$

where $A(x,z)$ is the y -component of the magnetic vector potential, corresponding to the field distribution (3):

$$A(x,z) = \beta^{-1}z^2 \sin \alpha \cos \alpha - |z^3|(\sin^2 \alpha \cos \alpha/3\beta^2) - x \sin \alpha \text{ for } |z| < \beta/\sin \alpha,$$

and

$$A(x,z) = |z| \cos \alpha - x \sin \alpha - (\beta \cos \alpha/3 \sin \alpha) \text{ for } |z| > \beta/\sin \alpha.$$

The two additive constants C_1 and C_2 are determined from the particle initial pitch angle θ_i and phase φ_i . Trajectory computations have been performed using a standard 4th-order Runge-Kutta procedure; in a test runs with $\beta = 100$ (almost adiabatic motion) the difference between final and initial pitch angles was found not to exceed $\Delta\theta = |\theta_f - \theta_i| \sim 0.05^\circ$. This provides sufficient accuracy and eliminates possible effects of numerical error accumulation.

4. RESULTS

Computations were carried out for several values of β and α in the range $0.05 \leq \beta \leq 30$ and $10^\circ \leq \alpha \leq 30^\circ$. Dependence of scattering effects on the angle α has been studied for $\beta = 0.2$ and $10^\circ \leq \alpha \leq 60^\circ$. The size of the matrix S_{ki} was chosen in most cases to be 20×20 , i.e. $\Delta\mu_f = \Delta\mu_i = 0.05$; from each of 20 μ_i intervals 1200 trajectories were computed giving thus a sufficient number of points in the final μ_f distribution to provide accurate determination of S_{ki} . Figure 2 shows three-dimensional displays of the $S(\mu_f, \mu_i)$ distributions for $\beta = 19$, $\alpha = 30^\circ$ (a), $\beta = 2$, $\alpha = 20^\circ$ (b), and $\beta = 0.1$, $\alpha = 20^\circ$ (c).

Solution of the integral equation (2) was obtained by its reduction to an algebraic system of 20 linear equations. The normalization condition, imposed on the kernel function

$$\int_0^1 S(\mu_f, \mu_i) d\mu_f = 1 \quad (4)$$

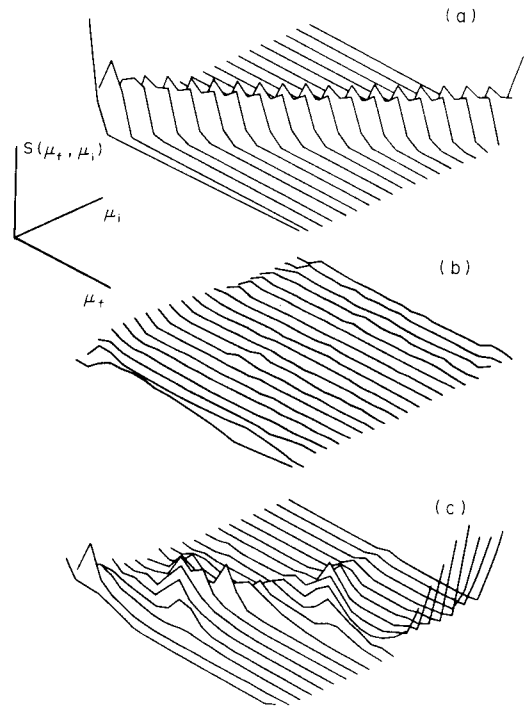


FIG. 2. THREE-DIMENSIONAL DISPLAYS OF THE $S(\mu_f, \mu_i)$ DISTRIBUTIONS FOR THREE VALUES OF THE REVERSAL REGION THICKNESS.

(a) A case of a comparatively weak scattering with $\beta = 19$, $\alpha = 30^\circ$. (b) A completely non-adiabatic case (strong scattering, isotropic distribution function) with $\beta = 2$, $\alpha = 20^\circ$. (c) Scattering in a thin current sheet with $\beta = 0.1$, $\alpha = 20^\circ$; anisotropic stationary distribution is formed in this case.

following from definition of the function S , guarantees solubility of the problem. The solutions obtained have been checked by substituting them in (2).

The main results of the computations will now be summarized. Throughout the interval $0.5 \leq \beta \leq 20$ the stationary distribution functions appear to be practically isotropic. For $\beta \leq 0.5$ a substantial anisotropy is found, its degree increasing rapidly as $\beta \rightarrow 0$. Four plots of stationary $f(\mu)$ are shown in Fig. 3, for $\beta = 15, 2, 0.2$ and 0.15 , from which a considerable increase in particle flux near $\theta \approx 90^\circ$ with adjacent depletion region is evident for the last two examples. For large values of β the scattering matrix tends to be close to the diagonal (Fig. 2a) and there arise some difficulties in obtaining the solution of (2) due to numerical instabilities. This feature is easy to understand from the obvious condition: $S(\mu_f, \mu_i) \rightarrow \delta(\mu_f - \mu_i)$, as $\beta \rightarrow \infty$ (no scattering), and, hence, any arbitrary

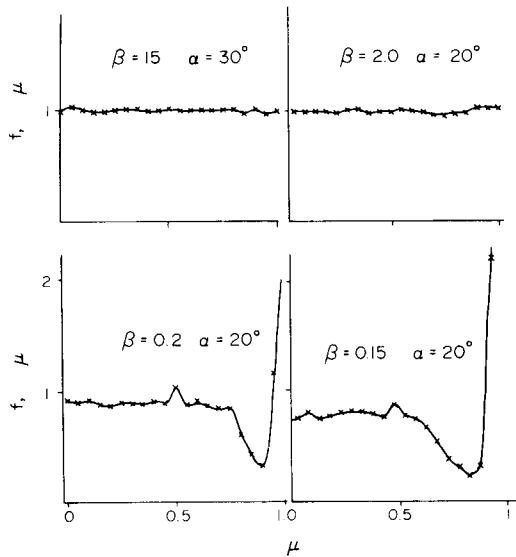


FIG. 3. STATIONARY DISTRIBUTION FUNCTIONS $f(u)$, CALCULATED FOR $\beta = 15, 2, 0.2$ AND 0.15 .

distribution function satisfies (2) in this limiting case. Consequently a considerable increase of size of the matrix S_{ki} is necessary for $\beta \geq 20$, requiring an unacceptably high amount of computer time.

An interesting feature of the $S(\mu_f, \mu_i)$ distributions for large β is their two-humped shape resulting from the fact that small pitch-angle scattering amplitudes appear to have a relatively low probability and, thus, for a uniform gyrophase distribution in the incident beam, a "fine structure" of peaks is formed, as can be seen in Fig. 2(a).

With regard to the dependence of particle scattering on the angle α , it was found, that for $\beta \geq 0.5$ the stationary distributions are insensitive to α and remain isotropic for $10^\circ \leq \alpha \leq 60^\circ$. For $\beta \leq 0.5$ the distribution functions tend to isotropy with increase of α , being anisotropic for smaller α values, thus, for $\beta = 0.2$ the distribution with $\alpha = 60^\circ$ is completely isotropic, whereas for $\alpha = 20^\circ$ we see a remarkable anisotropy (Fig. 3).

The characteristic relaxation time scale, τ , for setting the stationary distribution throughout a field line tube, depends on the efficiency of particle scattering in the reversal region, as well as on the average period of their oscillation between mirror points. Thus, distributions of particles with greater energies will reach the equilibrium state more rapidly. In the Earth's magnetotail the situation is much more complex, firstly, due to azimuthal drift

of particles, and, secondly, due to the large-scale magnetospheric convection. Note here, that in the framework of our simple magnetic field model with $\partial B/\partial x = 0$, in the limiting case of fully adiabatic motion ($\beta \gg 1$) particles should move along the drift-free orbits (Stern and Palmadesso, 1975). However, in reality the condition $\partial B/\partial x = 0$ is inapplicable to the near magnetotail region and, hence, for enough high energies the azimuthal drift velocity may be so large that the particle trajectory leaves the scattering zone in the magnetotail well before the substantial evolution of pitch-angle distribution could occur. In case $\beta \leq 10$, as can be seen from Fig. 2(b),(c), the scattering is so strong that τ is of the order of few bounce periods (seconds for 100 keV electrons, and a hundred of seconds for protons of the same energy). For greater values of β (lesser energies, and/or thicker current sheet, and/or greater B magnitude) we should expect much greater τ , since the scattering amplitude falls off very rapidly with rising β . A separate study for the case of small pitch angles ($\theta_i \approx 3^\circ$) and large β ($20 \leq \beta \leq 100$) has shown that with $\beta = 20$ and $\alpha = 25^\circ$ a typical pitch-angle scattering amplitude is $\sim 6^\circ$, whereas with $\beta = 60$ this quantity drops to $\sim 0.5^\circ$. The scattering amplitude decreases also with increasing angle α , because of lesser field line curvature for greater α values; in the investigated range $15^\circ \leq \alpha \leq 55^\circ$ an approximate relation applies: $\Delta\theta \sim (\sin \alpha)^{-1}$.

The results of this work can be applied to the investigation of particle precipitation in the ionospheric loss cone as well as to the drift loss cone filling in the region of the near magnetospheric tail, providing thus an interpretation of experimental data on the structure and dynamics of the particle precipitation zones and the stable trapping boundary. This question is beyond the scope of present paper and will be treated in a separate publication.

Acknowledgement—I am grateful to Dr. V. A. Sergeev for valuable discussions. It is also a pleasure to thank a referee for useful suggestions.

REFERENCES

- Pudovkin, M. I. and Tsyganenko, N. A. (1973). Particle motion and currents in the neutral sheet of the magnetospheric tail. *Planet. Space Sci.* **21**, 2027.
 Shabansky, V. P. (1971). Some processes in the magnetosphere. *Space Sci. Rev.* **12**, 299.
 Stern, D. P. and Palmadesso, P. (1975). Drift-free magnetic geometries in adiabatic motion. *J. geophys. Res.* **80**, 4244.

- Tsyganenko, N. A. (1975). On the adiabatic acceleration of auroral electrons by a transversal electric field. *Geomagn. Aeron.* **15**, 487.
- Tsyganenko, N. A. (1981). On the convective mechanism for formation of the plasma sheet in the magnetospheric tail. In *Magnetospheric Researches*, No. 2, publ. of Soviet Geophysical Comm., in press.
- Wagner, J. S., Kan, J. R. and Akasofu, S.-I. (1979). Particle dynamics in the plasma sheet. *J. geophys. Res.* **84**, 981.
- West H. I., Buck, R. M. and Kivelson, M. G. (1978). On the configuration of the magnetotail near midnight during quiet and weakly disturbed periods: magnetic field modeling. *J. geophys. Res.* **83**, 3819.